A more detailed comparison between experiment and theory will require an advanced theoretical calculation on $Fe^{II}(THF)_2TPP$ itself. It is clear that such a calculation is a challenge, even with the best computers available at present.

The temperature dependence of the Fe–O and Fe–N distances and the increase in magnetic moment below 60 K suggest that the ground state may be a function of temperature. However, the relative constancy of the Mössbauer results seems to rule out large changes in the electron distribution around the iron atom. We are presently making EXAFS measurements to examine the variability of the iron coordination sphere below liquid-nitrogen temperature.

Acknowledgment. Support of this work by the National Institutes of Health (Grants HL2388404 to P. Coppens and GM34073 and AM19856 to R. H. Blessing) and the National Science Foundation (Grant CHE8403428) is gratefully acknowledged.

Registry No. $Fe^{II}(THF)_2TPP$, 29189-60-4.

Supplementary Material Available: Listings of coefficients of least-squares planes, deviations from planes, and dihedral angles (4 pages); listing of observed and calculated structure factors (40 pages). Ordering information is given on any current masthead page.

Bis-Benzimidazole-Appended Binucleating Porphyrin Ligands: Synthesis, Characterization, and X-ray Structure

Nigel G. Larsen, Peter D. W. Boyd,[1] Steven J. Rodgers, Gerald E. Wuenschell, Carol A. Koch, Susan Rasmussen, John R. Tate, Brian S. Erler, and Christopher A. Reed*

Contribution from the Departments of Chemistry, University of Southern California, Los Angeles, California, 90089-1062, and University of Auckland, Auckland, New Zealand.
Received March 28, 1986

Abstract: The synthesis and characterization of some new binucleating tetraarylporphyrin ligands is reported. The potentially most useful example is α,α,5,15-bis[*N*-(2-methylbenzimidazolyl)acetamidophenyl]-α,α,10,20-bis(pivalamidophenyl)porphine (**8**). The ligands have two appended benzimidazole arms which are designed to chelate a second metal directly above the porphyrin. The synthetic methodology for obtaining both the 5,15 (i.e., trans) and the 5,10 (i.e., cis) bis-appended ligand from an α, α, α, α,5,10,15,20 *tetra*-functionalized starting material is described in detail. A key design feature of the ligand system is amenability to single-crystal X-ray structure determination and this is demonstrated with an X-ray structure of a copper(II) complex. Crystal data for $CuC_{74}H_{66}N_{12}O_4 \cdot 1.5$(diethyl ether)·toluene are the following: monoclinic, $C2/c$, a = 31.240 (4) Å, b = 16.769 (5) Å, c = 35.199 (4) Å, β = 121.4 (1)°; R = 0.0823, R_w = 0.0826. H bonding between the benzimidazole moieties and the pivalamido pickets is seen to determine the structural disposition of the appendages lying above the porphyrin ring. Iron(III) porphyrin complexes of these new ligands exist in a hydroxo monomer form as well as the familiar μ-oxo dimer form.

In the last decade the synthetic model approach to hemoprotein structure and reactivity has developed into a sophisticated art and a detailed science. Synthetic elaboration at the periphery of a tetrapyrrolic core has provided porphyrins with a wide array of useful appendages and superstructures. The aesthetic appeal of these structures has been captured in their nomenclature with descriptive terms such as cyclophane,[2] picket-fence,[3] chelated,[4] capped,[5] strapped,[6] basket-handle,[7] tail,[8,9] hanging base,[10] crowned,[11] bridged,[12] double,[13] pocket,[14,15] face-to-face,[16,17] cofacial,[18] strati,[19] gable,[20] caroteno,[21] tulip garden,[22] and lipid[23] porphyrins. A particular emphasis in the more recent work has been the construction of *binucleating* porphyrins which hold a pair of metals in close proximity.[11,16-20,24-33] Part of the motivation for this synthesis has been to model the structure[27,31,34,35] or the reactivity[36-38] of cytochrome oxidase[39] whose heterobinuclear heme/copper active site functions as nature's oxygen electrode. The rate and efficiency of cytochrome oxidase catalysis in the four-electron reduction of oxygen to water has proved to be very difficult to duplicate in man-made systems. A number of synthetically elegant porphyrins having appended ligands for binding a second metal have been reported, but a convincing structural model for the active site of cytochrome oxidase has yet to be characterized. The evolution of the model compound approach toward this goal requires first and foremost the unambiguous establishment of structure in binuclear systems. This essentially means single-crystal X-ray structure determination since the

* University of Southern California.

(1) University of Auckland.
(2) Diekmann, H.; Chang, C. K.; Traylor, T. G. *J. Am. Chem. Soc.* **1971**, *93*, 4068-4070. Traylor, T. G.; Tsuchiya, S.; Campbell, D.; Mitchell, M.; Stynes, D.; Koga, N. *J. Am. Chem. Soc.* **1985**, *107*, 604-614.
(3) Collman, J. P.; Gagne, R. R.; Reed, C. A.; Halbert, T. R.; Lang, G.; Robinson, W. T. *J. Am. Chem. Soc.* **1975**, *97*, 1427-1439.
(4) Chang, C. K.; Traylor, T. G. *Proc. Natl. Acad. Sci. U.S.A.* **1973**, *70*, 2647-2650. Geibel, J.; Cannon, J.; Campbell, D.; Traylor, T. G. *J. Am. Chem. Soc.* **1978**, *100*, 3575-3585.
(5) Almog, J.; Baldwin, J. E.; Crossley, M. J.; Debernardis, J. F.; Dyer, R. L.; Peters, M. K. *Tetrahedron* **1981**, *37*, 3589-3606.
(6) Baldwin, J. E.; Crossley, M. J.; Klose, T.; O'Rear, E. A., III; Peters, M. K. *Tetrahedron* **1981**, *38*, 27-39.
(7) Momenteau, M.; Loock, B.; Mispelter, J.; Bisagni, E. *Nouv. J. Chim.* **1979**, *3*, 77-79. Lavalette, D.; Tetreau, C.; Mispelter, J.; Momenteau, M.; Lhoste, J.-M. *Eur. J. Biochem.* **1984**, *145*, 555-565.
(8) Mashiko, T.; Reed, C. A.; Haller, K. J.; Kastner, M. E.; Scheidt, W. R. *J. Am. Chem. Soc.* **1981**, *103*, 5758-5767.
(9) Collman, J. P.; Brauman, J. I.; Doxsee, K. M.; Halbert, T. R.; Bunnenberg, E.; Linder, R. E.; LaMar, G. N.; Del Gaudio, J.; Lang, G.; Spartalian, K. *J. Am. Chem. Soc.* **1980**, *102*, 4182-4192.
(10) Momenteau, M.; Lavalette, D. *J. Chem. Soc., Chem. Commun.* **1982**, 341-343.
(11) Chang, C. K. *J. Am. Chem. Soc.* **1977**, *99*, 2819-2822.
(12) Battersby, A. R.; Buckley, D. G.; Hartley, S. G.; Turnball, M. D. *J. Chem. Soc., Chem. Commun.* **1976**, 879-881.
(13) Ogoshi, H.; Sugimoto, H.; Yoshida, Z. *Tetrahedron Lett.* **1977**, 169-172.

0002-7863/86/1508-6950$01.50/0

Scheme I. Synthetic Pathways to Ligand-Appended Porphyrins

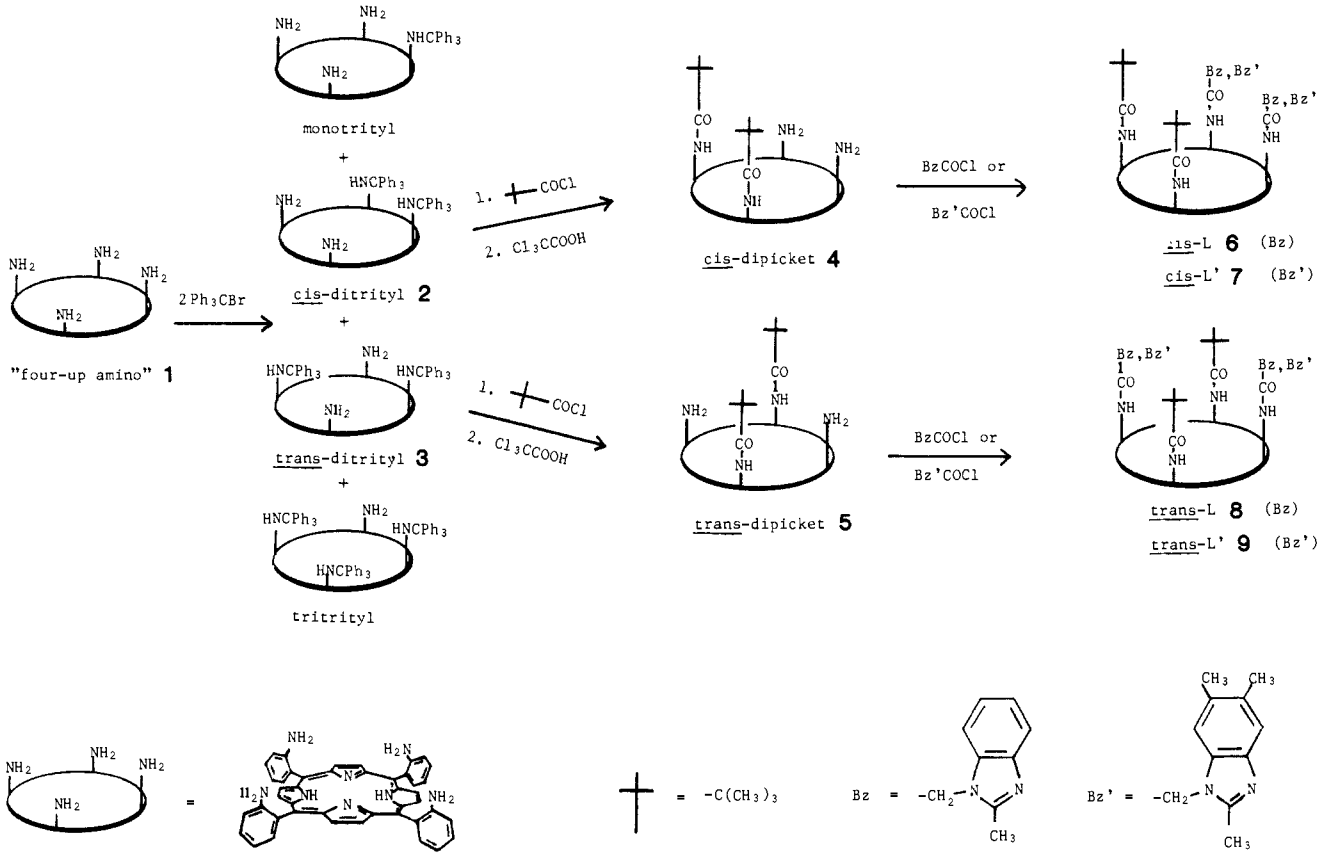

opportunity for error in assigning structure with complex ligands, particularly those with flexible appendages, is distressingly large. The power of ^{1}H NMR spectroscopy for characterizing the metal-free ligand is frequently diminished or completely lost in the presence of paramagnetic metals, particularly copper(II). Application of EPR spectroscopy can also be limited in magnetically coupled systems because of overall integral spin states. Building molecules with space-filling models is always useful but can be a seductive and deceptive guide to the structure of real molecules. A particular difficulty is distinguishing between intramolecular and intermolecular interactions in the solid state. Another common problem of binucleating systems is compound purity,[34,30] and this greatly hampers the definitive characterization of complex molecules, particularly when bulk properties such as magnetic susceptibility are being investigated. This, incidentally, may be a problem with the enzyme itself.[41]

In this paper we report the synthesis of a new ligand-appended porphyrin system, based on **8** (Scheme I), that has considerable binucleating potential. It contains two benzimidazole arms anchored trans to each other via *o*-amidophenyl linkages in the 5,15 positions of a porphyrin. The analogous cis compound having 5,10-benzimidazole appendages has also been synthesized. The virtues of *o*-amido functionalization of tetraarylporphyrins are well recognized. This is reflected in its extensive use in derivatized porphyrins. Tetra-[3] and monofunctionalization[14] have been widely exploited, but the apparently tedious problem of *di*functionalization of $\alpha,\alpha,\alpha,\alpha$-*tetra*arylporphyrins has not yet been approached. Hybrid diphenylporphyrins[29,31,42] are attractive alternatives, but

(14) Collman, J. P.; Brauman, J. I.; Collins, T. J.; Iverson, B.; Lang, G.; Pettman, R. B.; Sessler, J. L.; Walters, M. A. *J. Am. Chem. Soc.* **1983**, *105*, 3038–3052.
(15) Suslick, K. S.; Fox, M. M. *J. Am. Chem. Soc.* **1983**, *105*, 3507–3510.
(16) Collman, J. P.; Chong, A. O.; Jameson, G. B.; Oakley, R. T.; Rose, E.; Schmittou, E. R.; Ibers, J. A. *J. Am. Chem. Soc.* **1981**, *103*, 516–533.
(17) Landrum, J. T.; Grimmett, D.; Haller, K. J.; Scheidt, W. R.; Reed, C. A. *J. Am. Chem. Soc.* **1981**, *103*, 2640–2650.
(18) Netzel, T. L.; Bergkamp, M. A.; Chang, C. K. *J. Am. Chem. Soc.* **1982**, *104*, 1952–1957. Eaton, S. S.; Eaton, G. R.; Chang, C. K. *J. Am. Chem. Soc.* **1985**, *107*, 3177–3184.
(19) Kagan, N. E.; Mauzerall, D.; Merrifield, R. B. *J. Am. Chem. Soc.* **1977**, *99*, 5484–5486.
(20) Tabushi, I.; Sasaki, T. *J. Am. Chem. Soc.* **1983**, *105*, 2901–2902.
(21) Gust, D.; Moore, T. A.; Benasson, R. V.; Mathis, P.; Land, E.; Chachaty, C.; Moore, A. L.; Liddell, P. A.; Nemeth, G. A. *J. Am. Chem. Soc.* **1985**, *107*, 3631–3640.
(22) Takagi, S.; Miyamoto, T. K.; Sasaki, Y. *Bull. Chem. Soc. Jpn.* **1985**, *58*, 447–454.
(23) Tsuchida, E.; Nishida, H.; Yuasa, M.; Hasegawa, E.; Matsushito, Y.; Eshima, K. *J. Chem. Soc., Dalton Trans.* **1985**, 275–278.
(24) Elliott, M. C. *J. Chem. Soc., Chem. Commun.* **1978**, 399–400.
(25) Buckingham, D. A.; Gunter, M. J.; Mander, L. N. *J. Am. Chem. Soc.* **1978**, *100*, 2899–2901.
(26) Okamoto, M.; Nishida, Y.; Kida, S. *Chem. Lett.* (*Jpn.*) **1982**, 1773–1776.
(27) Chang, C. K.; Koo, M. S.; Ward, B. *J. Chem. Soc., Chem. Commun.* **1982**, 716–719.
(28) Hamilton, A. D.; Lehn, J.-M.; Sessler, J. L. *J. Chem. Soc., Chem. Commun.* **1984**, 311–313.
(29) Young, R.; Chang, C. K. *J. Am. Chem. Soc.* **1985**, *107*, 898–909.
(30) Hamilton, A. D.; Rubin, H.-D.; Bocarsly, A. B. *J. Am. Chem. Soc.* **1984**, *106*, 7255–7257.
(31) Gunter, M. J.; Mander, L. N.; Murray, K. S.; Clark, P. E. *J. Am. Chem. Soc.* **1981**, *103*, 6784–6787.
(32) Wasielewski, M. R.; Niemczyk, M. P.; Svec, W. A. *Tetrahedron Lett.* **1982**, *23*, 3215–3218.
(33) Dolphin, D.; Hiom, J.; Paine, J. B. *Heterocycles* **1981**, *16*, 417–447.
(34) Gunter, M. J.; Berry, K. J.; Murray, K. S. *J. Am. Chem. Soc.* **1984**, *106*, 4227–4235.
(35) Saxton, R. J.; Wilson, L. J. *J. Chem. Soc., Chem. Commun.* **1984**, 359–361.
(36) Durand, R. R.; Bencosme, C. S.; Collman, J. P.; Anson, F. C. *J. Am. Chem. Soc.* **1983**, *105*, 2710–2718.
(37) Chang, C. K.; Liu, H. Y.; Abdalmuhdi, I. *J. Am. Chem. Soc.* **1984**, *106*, 2725–2726.
(38) Gunter, M. J.; Mander, L. N.; Murray, K. S. *J. Chem. Soc., Chem. Commun.* **1981**, 799–801.
(39) Malmstrom, B. G. *Biochim. Biophys. Acta* **1979**, *549*, 281–303.
(40) Elliott, C. M.; Krebs, R. R. *J. Am. Chem. Soc.* **1982**, *104*, 4301–4303.
(41) Brudvig, G. W.; Stevens, T. H.; Morse, R. H.; Chan, S. I. *Biochemistry* **1981**, *20*, 3912–3921.
(42) Lecas, A.; Levisalles, J.; Renko, Z.; Rose, E. *Tetrahedron Lett.* **1984**, *25*, 1563–1566.

these molecules do not have the remaining difunctionality for further elaboration. In our ligands we incorporate two pivalamido moieties along with two benzimidazole appendages to act as steric blocking groups. This should favor discrete intramolecular chemistry over oligomeric complications. And not incidentally, it gives the system a greater capacity for variation and probably assists in crystallization of derivatives for X-ray structure determination. Our primary goal of showing that this ligand system is amenable to single-crystal X-ray crystallography has been achieved in the determination of the structure of a complex having copper(II) in the porphyrin. The binucleating capacity of the ligand's chelating superstructure, which would justify the name "pincer porphyrin", and the synthesis of models for cytochrome oxidase will be the subjects of future publications.

Experimental Section

General conditions for solvent purification and the handling of air-sensitive materials have been described previously.[17] NMR spectra were recorded on IBM WP270-SY or JEOL FX-90Q instrumentation. Column grade silica gel was EM (Merck) 100, 70–230 mesh and plc[43] grade was 60 PF254 (Merck 7747). Elemental analyses and FAB-Mass Spectra were performed at the U.C. Berkeley Microanalytical Laboratory. $\alpha,\alpha,\alpha,\alpha$-*meso*-Tetrakis(*o*-aminophenyl)porphyrin (**1**) was prepared in the usual manner,[3,44] and the yield of the $\alpha,\alpha,\alpha,\alpha$ isomer was increased by a silica gel reflux process.[45,46] Dimethylformamide[43] was freshly vacuum distilled from BaO onto 4 Å molecular sieves. Thionyl chloride was distilled from triphenyl phosphite. Dichloromethane was dried over 4 Å molecular sieves. Thin-layer chromatography was performed on Analtech Silica Gel GF plates. All other reagents were commercially available and used without further purification unless otherwise noted.

Characterization of Pivaloyl Picket Porphyrin Mixture. $\alpha,\alpha,\alpha,\alpha$-*meso*-Tetrakis(*o*-aminophenyl)porphyrin, **1**, (4.0 g, 5.9 mmol) was dissolved in dry dichloromethane (100 mL) and pyridine (1 mL) and cooled in an ice bath. Pivaloyl chloride (1.46 mL, 0.012 mol) in CH_2Cl_2 (50 mL) was added dropwise over about 90 min, and the mixture was allowed to warm over a 2-h period. The solution was then washed with 100-mL portions of dilute aqueous ammonium hydroxide then water and dried over Na_2SO_4. The product (4.12 g) was crystallized out by addition of methanol and stripping of solvent on a rotary evaporator. Twice-eluted TLC on silica gel with 6:1:1 $CHCl_3$/ether/hexanes showed the presence of five separable species, one of which was later deduced to have two components. The identity of all six components of the mixture was obtained by TLC comparison to known compounds, by ^1H NMR and by independent synthesis of the cis and trans dipicket species as described in the text. Crude separation by column chromatography on plc grade silica gel with 6:1 $CHCl_3$/ether gave the first and major fraction as a mixture of tetra-, tri-, cis and trans dipicket species. The second fraction was monopicket. Final elution with 1:1 acetone/ether gave starting material **1**.

Trans-Dipicket 5. To a reaction vessel charged with **1** (10.0 g, 14.8 mmol), pyridine (5.0 mL, 62 mmol), and anhydrous K_2CO_3 (10.0 g, 72 mmol) in dichloromethane (1.2 L) at 0 °C was added dropwise over 4 h a solution of trityl bromide (9.40 g, 29.1 mmol) in 200 mL of CH_2Cl_2 under N_2. The reaction mixture was stirred an additional 2 h and then washed with 10% NH_4OH (2 × 1 L) and H_2O (2 × 1 L) and dried (Na_2SO_4). After removal of the solvent and drying in vacuo overnight, the residue was dissolved in dichloromethane, 150 mL of Silica Gel 100 was added, and the solvent was removed under vacuum. The loaded silica gel was applied to the top of a Silica Gel 100 column (heptane packed, 5 in. × 18 in.).

Elution with 9:1 and then 7:3 hexanes/EtOAc afforded three major bands, whose solvents were removed under vacuum (with addition of MeOH toward the end) and dried in vacuo overnight. The first band is a mixture of tritrityl and *trans*-ditrityl species, **3** (8.0 g, R_f 0.69 [7:3 hexanes/EtOAc]). The second band is *cis*-ditrityl species **2** (4.2 g, 24%, R_f 0.47 [7:3 hexanes/EtOAc], ^1H NMR (270 MHz, $CDCl_3$) δ −2.70 (s, 2 H), 3.60 (s, 4 H), 5.13 (s, 2 H), 6.7–8.0 (m, 57 H), 8.80 (s, 2 H), 8.9 (s, 2 H), 9.0 (d, 2 H), 9.07 (d, 2 H)). The third band is the previously reported monotrityl species.[14]

To the tritrityl/*trans*-ditrityl species mixture dissolved in dichloromethane (1 L) and pyridine (10.0 mL, 123 mmol) at 0 °C under N_2 was added dropwise over 30 min a solution of pivaloyl chloride (10.0 mL, 81 mmol) in 200 mL of dichloromethane. After being stirred for 4 h, the reaction mixture was washed with 0.3 M HCl (2 × 500 mL), 10% NH_4OH (2 × 500 mL), and H_2O (2 × 500 mL) and dried (Na_2SO_4), and the solvent was removed in vacuo.

The residue dissolved in dichloromethane (800 mL) was stirred with trichloroacetic acid (10 g, 61 mmol) at 0 °C under N_2 for 3 h. After being washed with 10% NH_4OH (2 × 1 L), H_2O (2 × 1 L), the solution was dried (Na_2SO_4) and the solvent removed.

Chromatography on a plc grade silica gel column (3 in. × 15 in.) eluted with $CHCl_3$ and then 6:1 $CHCl_3$/ether had two major bands, the second of which is the previously known monopicket.[14] Removal of the solvent from the first band and crystallization by rotoevaporation of a dichloromethane/MeOH solution of the residue afforded 3.17 g (25% yield from **1**) of *trans*-dipicket **5** as a microcrystalline purple solid. R_f 0.42 (3% MeOH/$CHCl_3$). ^1H NMR (270 MHz, $CDCl_3$) δ −2.64 (s, 2 H), 0.28 (s, 18 H), 3.54 (s, 4 H), 7.1–8.0 (m, 16 H), 8.71 (d, 2 H, J = 8.6 Hz), 8.79 (d, 4 H, J = 4.9 Hz), 8.90 (d, 4 H, J = 4.8 Hz). Anal. Calcd for $C_{54}H_{50}N_8O_2 \cdot H_2O$: C, 75.32; H, 6.09; N, 13.01. Found: C, 75.08; H, 5.77; N, 13.08.

Cis-Dipicket 4. This was prepared in an identical manner (proportionally scaled) as the trans-dipicket by acylation and detritylation of the *cis*-ditrityl fraction isolated as band no. 2 from the column of mixed-trityl products above. Thus, from pure *cis*-ditrityl **2** (3.00 g, 2.6 mmol) was isolated after identical chromatography and crystallization pure cis-dipicket **4**, 1.70 g (76% from *cis*-ditrityl, 18% from **1**), as a purple microcrystalline solid. R_f 0.42 (3% MeOH/$CHCl_3$). ^1H NMR (270 MHz, $CDCl_3$) δ −2.65 (s, 2 H), 0.14 (s, 18 H), 3.62 (s, 4 H), 7.0–8.0 (m, 16 H), 8.7–9.0 (m, 10 H). Anal. Calcd for $C_{54}H_{50}N_8O_2 \cdot H_2O$: C, 75.32; H, 6.09; N, 13.01. Found: C, 75.07; H, 6.06; N, 12.87.

Methyl 2-[*N*-(2-Methylbenzimidazolyl)]acetate. In a drybox, 2-methylbenzimidazole (20 g, 0.151 mol) was stirred with sodium hydride (3.63 g, 0.151 mol, dewaxed) in tetrahydrofuran (200 mL) for 3 h. The serum-stoppered flask was removed from the drybox and methyl 2-bromoacetate (12.68 mL, 0.151 mol) was added dropwise over 15 min. After 1 h of heating to reflux the reaction mixture was cooled and chloroform (100 mL) was added. The precipitate of NaBr was filtered off and the solvent evaporated to give an off-white solid of the crude methyl ester of 2-[*N*-(2-methylbenzimidazolyl)]acetic acid (28.3 g, 92%). ^1H NMR (90 MHz, $CDCl_3$): δ 2.57 (s, 3 H), 3.76 (s, 3 H), 4.81 (s, 2 H), 7.2 (m, 3 H), 7.7 (m, 1 H).

2-[*N*-(2-Methylbenzimidazolyl)]acetic Acid. Methyl 2-[*N*-(2-methylbenzimidazolyl)]acetate (10 g) was hydrolyzed by heating to reflux in 48% aqueous HBr (200 mL) for 30 min. The solvent was evaporated under reduced pressure to give a yellowish oil which was pumped under vacuum overnight. The oil was dissolved in a minimum amount of methanol, and chloroform (50 mL) was added. Anhydrous diethyl ether was added to the point of cloudiness, and upon cooling to dry ice temperatures the white hydrobromide salt of the acid crystallized out. This was collected by filtration and washed with cold ether. Recrystallization from methanol/chloroform/ether gave 10.1 g of final product (76%); *m/e* 190.1 corresponding to 2-[*N*-(2-methylbenzimidazolyl)]-acetic acid. ^1H NMR (90 MHz, Me_2SO-d_6): δ 2.85 (s, 3 H), 5.50 (s, 2 H), 7.5–8.0 (m, 4 H). Anal. Calcd for $C_{10}H_{10}N_2O_2 \cdot HBr$: C, 44.30; H, 4.09; N, 10.33; Br, 29.47. Found: C, 44.39; H, 4.11; N, 10.29; Br, 29.29. This hydrobromide salt was used as required for in situ generation of the acid chloride.

***trans*-L 8.** In a typical experiment a well-dried sample of 2-[*N*-(2-methylbenzimidazolyl)]acetic acid (2.52 g, 9.30 mmol) was dissolved in freshly distilled DMF (150 mL) in an oven-dried round-bottomed flask and treated with freshly distilled thionyl chloride (0.66 mL, 9.05 mmol) for 1 h at room temperature under N_2. The resulting orange-red solution of the acid chloride was used without isolation.

Well-dried trans-dipicket **5** (2.10 g, 2.44 mmol) and pyridine (distilled from KOH onto 4 Å molecular sieves, 6.0 mL) were added to the DMF solution of 2-[*N*-(2-methylbenzimidazolyl]acetyl chloride, and the reaction mixture was stirred overnight at room temperature under N_2. After the addition of 300 mL of dichloromethane, the reaction mixture was washed with 0.1 M HCl (3 × 300 mL), 10% NH_4OH (3 × 300 mL), and saturated aqueous NaCl (5 × 300 mL) and then dried (Na_2SO_4), and the solvent was removed under vacuum. The purple solid was applied in $CHCl_3$ to a plc grade silica gel column (2.5 in. × 10 in.) and flash eluted with $CHCl_3$ and then 2% MeOH/$CHCl_3$. Impure fractions were combined and rechromatographed. After removal of the solvent, the combined pure fractions were dissolved in dichloromethane and filtered though a fine frit. An equal volume of MeOH was added, and the solvents were removed under vacuum, yielding 2.82 g (96%) of a microcrystalline purple solid. R_f 0.30 (3% MeOH/$CHCl_3$). ^1H NMR (270 MHz, $CDCl_3$): δ −2.69 (s, 2 H), −1.61 (s, 6 H), 0.28 (s, 18 H), 3.98 (s, 4 H), 7.0–8.7 (m, 34 H), 9.75 (s, 2 H). Anal. Calcd for $C_{74}H_{66}N_{12}O_4 \cdot H_2O$: C, 73.73; H, 5.69; N, 13.94. Found: C, 73.88; H,

(43) Abbreviations: THF = tetrahydrofuran; DMF = *N*,*N*-dimethylformamide; Me_2SO = dimethyl sulfoxide; TPP = tetraphenylporphinato dianion; plc = preparative layer chromatography.
(44) Sorrell, T. N. *Inorg. Synth.* **1980**, *20*, 161–169.
(45) Lindsey, J. *J. Org. Chem.* **1980**, *45*, 5215.
(46) Elliott, C. M. *Anal. Chem.* **1980**, *52*, 666–668.

5.53; N, 14.01. FAB-mass spectrum 1187 (M + H), 1129, 1041.

***cis*-L 6.** This was synthesized by two routes. Coupling of the appropriate benzimidazole acid chloride (see below) with pure cis-dipicket **4** afforded *cis*-L **6** directly. However, from the standpoint of synthetic ease and yield the method of choice is to take the first band off a crude column after acylation of **1** with pivaloyl chloride (a mixture of four components, see above) and treat this directly with the appropriate benzimidazole acid chloride. A mixture of cis- and trans-dipicket, tripicket, and tetrapicket species (1.0 g) was treated at 0 °C with an excess of the 2-[*N*-(2-methylbenzimidazolyl)]acetyl chloride solution obtained above. The solution was left to stir overnight and allowed to warm to room temperature. Dichloromethane (300 mL) was added, and the reaction mixture was extracted with dilute ammonium hydroxide followed by several washings with water. Dilute saline washes were used in cases of emulsion formation. After the dichloromethane solution was dried with Na_2SO_4 the solvent was removed under reduced pressure and the residue was dried in vacuo overnight to remove remaining traces of DMF. The product was recrystallized from $CHCl_3$/methanol before chromatographing on plc grade silica gel eluting with 6:1 $CHCl_3$/ether and then 30:5:1 $CHCl_3$/ether/methanol. The fourth and major band was the desired *cis*-L ligand, **6**, and it was isolated as purple crystals from $CHCl_3$/methanol (0.38 g, R_f 0.23 (3% MeOH/$CHCl_3$)). Anal. Calcd for $C_{74}H_{66}N_{12}O_4 \cdot H_2O$: C, 73.37; H, 5.69; N, 13.94. Found: C, 72.96; H, 5.73; N, 13.81. ^1H NMR (270 MHz, $CDCl_3$): δ −3.01, (s, 2 H), 0.47 (s, 18 H), 1.60 (s, 6 H + H_2O), 4.11 (s, 4 H), 5.24 (br m, 2 H), 5.42 (br m, 2 H), 5.97 (br m, 2 H), 6.31 (d, 2 H), 7.4–8.9 (m, 26 H), 9.23 (br s, 2 H).

Methyl 2-[*N*-(2,5,6-Trimethylbenzimidazolyl)]acetate. 2,5,6-Trimethylbenzimidazole[47] (20 g, 0.125 mol) was added in small aliquots under nitrogen to a dry THF solution (200 mL) of dewaxed NaH (3.63 g, 0.15 mol), and the reaction was stirred for 3 h. Methyl 2-bromoacetate (12.68 mL, 0.151 mol) in several milliliters of THF was added dropwise over 15 min. The solution was heated to reflux overnight and cooled, and $CHCl_3$ (100 mL) was added. The precipitate of NaBr was removed by filtration and the solvent volume reduced on a rotary evaporator. Diethyl ether was added, and upon further stripping of solvent the white crystalline ester (13.3 g) was deposited in 46% yield. ^1H NMR (90 MHz, $CDCl_3$): δ 2.35 (s, 6 H), 2.52 (s, 3 H), 3.75 (s, 3 H), 4.76 (s, 2 H), 6.94 (s, 1 H), 7.43 (s, 1 H).

2-[*N*-(2,5,6-Trimethylbenzimidazolyl)]acetic Acid. Methyl 2-[*N*-(2,5,6-trimethylbenzimidazolyl)]acetate (10 g, 0.045 mol) was hydrolyzed to the corresponding acid with HBr (200 mL) in a similar manner as described above except that longer reflux time (2 h) was required. The yield of hybrobromide salt was 9.9 g (73%). ^1H NMR (90 MHz, Me_2SO-d_6): δ 2.45 (s, 6 H), 2.80 (s, 3 H), 5.38 (s, 2 H), 7.52 (s, 1 H), 7.58 (s, 1 H).

***trans*-L′ 9.** The in situ preparation of 2-[*N*-(2,5,6-trimethylbenzimidazolyl)]acetyl chloride needed for this ligand synthesis was prepared as follows. In a typical preparation the hydrobromide salt of 2-[*N*-(2,5,6-trimethylbenzimidazolyl)]acetic acid (0.50 g, 1.67 mmol) was suspended in about 25 mL of dry dichloromethane, and thionyl chloride (0.12 mL, 1.67 mmol) and DMF (ca. 4 drops) were added. The mixture was stirred overnight after which time the solid dissolved to give an orange solution which was ready for use.

A dichloromethane solution of trans-dipicket **5** (0.20 g, 0.25 mmol) was added to the dichloromethane solution of 2-[*N*-(2,5,6-trimethylbenzimidazolyl)]acetyl chloride maintained at 0 °C. Pyridine (ca. 1 mL) was added until the solution color changed from green to red. The reaction mixture was stirred for 2 h and then washed first with dilute ammonium hydroxide then water, dilute hydrochloric acid, water, dilute ammonium hydroxide again, and finally water at least twice. The resulting dichloromethane solution was dried with anhydrous Na_2SO_4, and the solvent was evaporated under reduced pressure. The product was purified by chromatography on a 2 × 10 cm column of plc grade silica gel eluting with 4:3:3 dichloromethane/ether/hexanes. The desired major fraction was preceded by some minor components. Crystallization from dichloromethane/pentane gave **9** (0.237 g, 75%). Anal. Calcd for $C_{78}H_{74}N_{12}O_4 \cdot H_2O$: C, 74.25; H, 6.08; N, 13.32. Found: C, 74.54; H, 5.83; N, 13.21. ^1H NMR (270 MHz, $CDCl_3$): δ −2.70 (s, 2 H), −1.70 (s, 6 H), 0.25 (s, 18 H), 2.28 (s, 6 H), 2.36 (s, 6 H), 3.91 (s, 4 H), 6.9–8.7 (m, 30 H), 9.79 (s, 2 H).

***cis*-L′ 7.** This was prepared in an analogous manner to *cis*-L **6** and characterized by ^1H NMR (100 MHz, $CDCl_3$): δ −2.62 (s, 2 H), −0.24 (s, 6 H), 0.29 (s, 18 H), 2.04 (s, 6 H), 2.09 (s, 6 H), 3.83 (d, 2 H), 4.07 (d, 2 H), 6.74 (s, 2 H), 6.94 (s, 2 H), 7.34–9.23 (m, 28 H).

Iron–Porphyrin Complexes. Iron insertions were carried out by anaerobic treatment of the appropriate ligand with excess $FeBr_2$ in 1:1 THF/benzene in the presence of K_2CO_3. In a typical experiment *cis*-L **6** (0.4 g), $FeBr_2$ (0.4 g), and K_2CO_3 (0.1 g) were stirred in 1:1 benzene/THF (60 mL) at room temperature overnight. The reaction was monitored spectrophotometrically by following the formation of a *symmetrical* 540-nm band presumed to be due to a mono- or bis-THF complex of iron(II). The reaction mixture was worked up aerobically by removal of the solvents under reduced pressure and extraction of the dark residue with CH_2Cl_2. These extracts were concentrated and washed first with dilute aqueous HBr (2 × 50 mL), H_2O (2 × 50 mL), concentrated NH_4OH (2 × 100 mL), H_2O (2 × 100 mL), concentrated aqueous sodium citrate (2 × 100 mL), and H_2O (2 × 100 mL). The CH_2Cl_2 solution was dried over sodium sulfate, and the black microcrystalline product was produced by addition of heptane (0.35 g, 84%); $\mu_{eff}^{300K} = 4.2$ μ_B. Anal. Calcd for $C_{148}H_{128}N_{24}O_9Fe_2 \cdot 4H_2O$: C, 69.15; H, 5.33; N, 13.08. Found: C, 69.36; H, 5.56; N, 12.65. IR (KBr) ν(Fe–O) = 865 cm^{-1} (s). TLC on silica gel eluting with 30:5:1 $CHCl_3$/ether/methanol revealed two closely separated components. Column chromatography on PLC grade silica gel eluting with the same solvent mixture gave a partial separation. By fractional collection and rapid isolation, spectroscopically distinct fractions were collected. The fastest moving band was assumed to be Fe(OH)(*cis*-L). It had virtually no IR (KBr) absorption at 865 cm^{-1} and its UV-VIS spectrum had λ_{max} at 625 sh, 578, and 421. The slower moving band was assumed to be the μ-oxo dimer Fe_2O(*cis*-L)$_2$. It had a strong IR (KBr) band at 865 cm^{-1} and its UV–vis spectrum had λ_{max} (610, 570, 415) and band shapes essentially identical with Fe_2O(TPP)$_2$ (610, 570, 412).

Cu(*trans*-L′). Ligand **9** (0.174 g, 0.138 mmol) was dissolved in $CHCl_3$ (25 mL) and mixed with $Cu(OAc)_2 \cdot H_2O$ (0.061 g, 0.306 mmol) dissolved in methanol (15 mL). After the mixture was stirred for 15 min, the solvents were removed under reduced pressure. The product was dissolved in dichloromethane and filtered through a fine frit. Plc grade silica gel was added to the solution, the solvent was evaporated, and the product was loaded onto a 2 × 4.5 cm column packed with heptane. Elution with 4% methanol in chloroform gave one major band which was collected and vapor diffused with pentane to give purple crystals of a trichloroform solvate (0.158 g, 69%). Anal. Calcd for $C_{78}H_{72}N_{12}O_4Cu \cdot {}^1/_3CHCl_3$: C, 58.49; H, 4.55; N, 10.11; Cl, 19.18; Cu, 3.82. Found: C, 58.74; H, 4.50; N, 10.20; Cl, 18.49; Cu 3.95.

Cu(*trans*-L). Ligand **8** (0.500 g, 0.415 mmol) dissolved in $CHCl_3$ (100 mL) was mixed with $Cu(OAc)_2 \cdot H_2O$ (0.165 g, 0.829 mmol) dissolved in MeOH (50 mL). After the mixture was stirred overnight and the solvents removed, the residue was suspended in a small amount of CH_2Cl_2, filtered in a fine frit, and the solvent was removed. The product was applied as a $CHCl_3$ solution to plc grade silica gel column (1.5 in. × 6 in.) and flask eluted with $CHCl_3$ first to remove two minor bands and then with 0.5% MeOH/$CHCl_3$. After removal of the solvent from the product fractions, the residue was dissolved in $CHCl_3$ and vapor diffused with pentane. Isolation and air drying afforded 0.484 g (91%) of purple crystals. Anal. Calcd for $C_{74}H_{64}N_{12}O_4Cu \cdot {}^1/_3CHCl_3$: C, 69.27; H, 5.03; N, 13.04; Cu, 4.93; Cl, 2.75. Found: C, 69.36; H, 5.02; N, 13.29; Cu, 4.98; Cl, 2.52. FAB-mass spectrum 1248, 1249 (M + H), 1190. X-ray quality single crystals were grown by vapor diffusion of diethyl ether into a toluene solution at 0 °C.

X-ray Structure Determination. Crystals of Cu(*trans*-L)·$1.5C_4H_{10}O \cdot C_7H_8$ were found to rapidly lose crystallinity upon separation from the mother liquor. Accordingly, selected crystals were mounted in thin-wall capillary tubes along with a small amount of the crystallizing liquid. A suitably diffracting crystal was found after several attempts, and intensity data were collected on a Nonius CAD4 diffractometer with

Table I. Crystal Data Collection and Refinement Data for Cu(*trans*-L)·$1.5C_4H_9O \cdot C_7H_8$

chemical formula	$CuC_{87}H_{89}N_{12}O_{5.5}$
crystal system	monoclinic
space group	$C2/c$
a, Å	31.240 (4)
b, Å	16.769 (5)
c, Å	35.199 (4)
β, deg	121.4 (1)
V, Å^3	15738.98 (10)
Z	8
μ, cm^{-1}	3.46
ρ(calcd), g cm^{-3}	1.068
radiation	Mo Kα 0.71073 Å
2θ scan range, deg/min	4–38
data collected	6792
unique reflcns ($F_o^2 > 2\sigma(F_o^2)$)	2435
R, R_w	0.0823, 0.0826

(47) Beaven, G. R.; Holiday, E. R.; Johnson, E. A.; Ellis, B.; Mamalis, P.; Petrow, V.; Sturgeon, B. *J. Pharm. Pharmacol.* **1949**, *1*, 957–970.

Zr filtered Mo Kα radiation with $2\theta/\omega$ scans. The stability of the crystal was checked by measurement of three standard reflections every 100 reflections, and no significant variation was observed. The data were corrected for Lorentz–polarization and absorption effects. Details of the crystal data collection are given in Table I.

The cell symmetry and systematic absences in the data set were consistent with space groups $C2/c$ or Cc. The space group $C2/c$ was assumed initially and confirmed by successful solution and refinement of the structure. The position of the central copper atom was determined from a sharpened Patterson synthesis. The positions of the remaining non-hydrogen atoms of the porphyrin were determined by difference Fourier maps combined with cycles of least-squares refinement. When all atoms of the ligand were found, several cycles of least-squares refinement were performed with anisotropic thermal parameters for the copper atom and coordination nitrogen atoms and isotropic thermal parameters for the remaining atoms. This led to values of R and R_w of 0.187 and 0.176 for $F_o^2 > \sigma(F_o^2)$. Three sets of peaks of height greater than 1 e/Å^3 were found in the final difference Fourier map. Two of these sets correspond to ether molecules of crystallization and the third to a toluene molecule. Further refinement of the structure was continued with the inclusion of these solvent molecules with block refinement. It then became clear that the solvent molecules needed restraint during least-squares refinement. Thus, the final scattering model used in the structure refinement included calculated positions for all hydrogen atoms on the pyrrole, phenyl, and benzimidazole rings and on the amide nitrogen atoms. The phenyl ring of the toluene solvate was refined as a rigid group. The methyl group of the toluene molecule together with the ether molecules were constrained to geometries near those reported for these molecules.[48] This model converged after three complete cycles of block refinement with final values of R and R_w of 0.0823 and 0.0826, respectively, for $F_c^2 > 2\sigma(F_o^2)$ where the final function minimized was $\Sigma\omega(|F_o| - |F_c|^2)$ with $\omega = 1.6186/(\sigma^2(F_o) + 0.00163(F_o^2)$. All calculations used in the structure solution and refinement were performed with SHELX programs on the Auckland University IBM 4341 computer. A final difference Fourier map was essentially featureless with a few peaks with heights <0.4 e/Å$^+$. A table of observed and calculated structure factors is given in the supplementary material.

Results and Discussion

Synthesis of the Ligands. The synthesis of the bis-benzimidazole-appended ligands begins with the familiar $\alpha,\alpha,\alpha,\alpha$-*meso*-tetrakis(*o*-aminophenyl)porphyrin, **1** (see Scheme I), known colloquially as "four-up amino". It was prepared in the usual manner,[3,44] and its yield was optimized by the silica gel reflux enrichment process.[45,46] The four-up atropisomeric nature of an ortho-substituted tetraaryl porphyrin such as **1** provides a versatile construction template upon which to build a ligating superstructure. The basic task was to find a way of appending functionality to only two of the four amino groups and then to determine whether this had occurred in cis (i.e., 5,10) or trans (i.e., 5,15) sites. Two appended ligands rather than four are ultimately more desirable for the long-term goal of obtaining models for cytochrome oxidase because tetrafunctionalization traps a chelated copper(II) in an essentially noninteracting manner above the porphyrin.[34] A trans arrangement of the two appended ligands is more desirable than a cis arrangement because a chelated metal would then be positioned more or less directly above a metal in the porphyrin. Blocking the two remaining *o*-amino groups with *tert*-butyl pickets was deemed desirable to help isolate the "active site" region and discourage intermolecular chemistry. The synthesis of 5,15 *o*-aminophenyl porphyrins without blocking picket substituents has been developed recently in three separate reports.[29,31,42]

The steric blocking effect of a *tert*-butyl group on an *o*-pivalamido substituent unfortunately offers no bias toward trans diacylation of **1**. Thus, when the four-up amino, **1**, is treated with 2–3 equiv of pivaloyl chloride the desired trans-dipicket is only a minor component of the resulting mixture of products. This is an expected result if acylation occurs in a kinetically determined random fashion since statistically cis acylation should occur twice as frequently as trans. In actual fact, all five possible acylated products are formed along with some unreacted **1**. The first band off a well-resolved column is the familiar picket-fence porphyrin[3] which we will refer to as tetrapicket. The second fastest moving fraction is the tripicket species, *meso*-α-mono(*o*-aminophenyl)-α,α,α-tri(*o*-pivalamidophenyl)porphyrin which has also been reported previously.[9] The third band required an alternative synthesis (vide infra) to identify its two components: the desired cis and trans dipicket species (**4** and **5**, respectively, in Scheme I). The fourth band was well resolved and was shown to be the previously reported[14] monopicket species. The cis- and trans-dipicket species have proved to be chromatographically inseparable in our hands, despite extensive efforts. This necessitated the development of the trityl procedure outlined below. Once separated, the pure cis- and trans-dipicket species can be readily distinguished by the greater pyrrole region symmetry in the trans isomer. Corroborating evidence that the cis- and trans-dipicket species are correctly identified comes from studies with the trityl-protected intermediates discussed below, and ultimate proof comes from X-ray crystallography on a copper complex of the ligand derived from the trans product. The difficulty of the separation described above and the fact that cis-diacylation is favored over trans by a factor of 2 makes direct acylation an impractical route to the most desired trans ligand. However, because the cis ligand was required in lesser amounts and also because separation from the trans was possible at the final stage we did in fact use this direct acylation method to obtain the cis ligand **6**.

A practical route to the desired trans dipicket was developed with trityl protecting groups. Trityl bromide is known[14] to react with the tetra-*o*-amino porphyrin **1** to form a secondary amine which is readily detritylated with acid. This chemistry can be carried out quickly at 0 °C so that any atropisomerism of the four-up isomer of the porphyrin is avoided. We anticipated that the steric bulk of the trityl group would favor trans difunctionalization over cis as well as inhibit tri- and possibly tetrafunctionalization. Yield measurements from the tritylation reactions described below indicate that these expectations were justified. Moreover, the tritylated products, particularly the cis- and trans-ditritylated products, are much more easily separated by chromatography than the acylated products, and this has led to a practical synthesis of the trans ligands. In addition, some of the unneeded tritylated products can be conveniently recycled by acid cleavage back to "four-up amino" starting material, thereby milking the system for additional yield.

The successful synthesis is outlined in Scheme I. Treatment of four-up amino, **1**, with 2 equiv of trityl bromide gave four major products which were readily separable into three major bands on silica gel column chromatography. The slowest moving band was shown to be the known[14] monotritylated species. The middle band was shown by ^{1}H NMR and also by subsequent acylation and trityl cleavage to be the *cis*-ditrityl product **2**. The fastest moving band (and major fraction) was shown to be an approximately 3:1 mixture of the desired *trans*-ditrityl product **3** and the tritritylated species. In practice, the chromatographic separation of this pair was most easily achieved after acylation of the mixture with pivaloyl chloride and acid cleavage of the trityl group. The resulting trans-dipicket **5** is produced in greater abundance than the cis isomer **4** by a ratio of approximately 4:3. Statistically, a reversed ratio of abundances is expected (theoretically 1:2) so the bulky trityl protecting group has effected an approximate threefold enhancement of the yield of trans over cis. The overall yield of trans-dipicket **5**, based upon four-up amino **1**, is 25%.

Treatment of the trans-dipicket species **5** with *N*-(2-methylbenzimidazole)acetyl chloride gave the trans bis-benzimidazole-appended ligand **8**. We refer to this ligand as *trans*-L and to the cis analogue **6** as *cis*-L. A minor change was made to the benzimidazole to give the very closely related pair of ligands *cis*-L′ **7** and *trans*-L′ **9**, where a 2,5,6-trimethyl-substituted benzimidazole has replaced the 2-methylbenzimidazole. This was done to see how two additional methyl groups might affect the solubility and crystallizability of the ligand system and its complexes. Figure 1 shows 270-MHz ^{1}H NMR spectra of the *cis*- and *trans*-L ligands **6** and **8**. Comparison of these spectra reveals two gross differences which must reflect different orientations of the 2-methylbenz-

(48) Andre, D.; Fourme, R.; Zeichmeister, K. *Acta Crystallogr.* **1972**, *B28*, 2389.

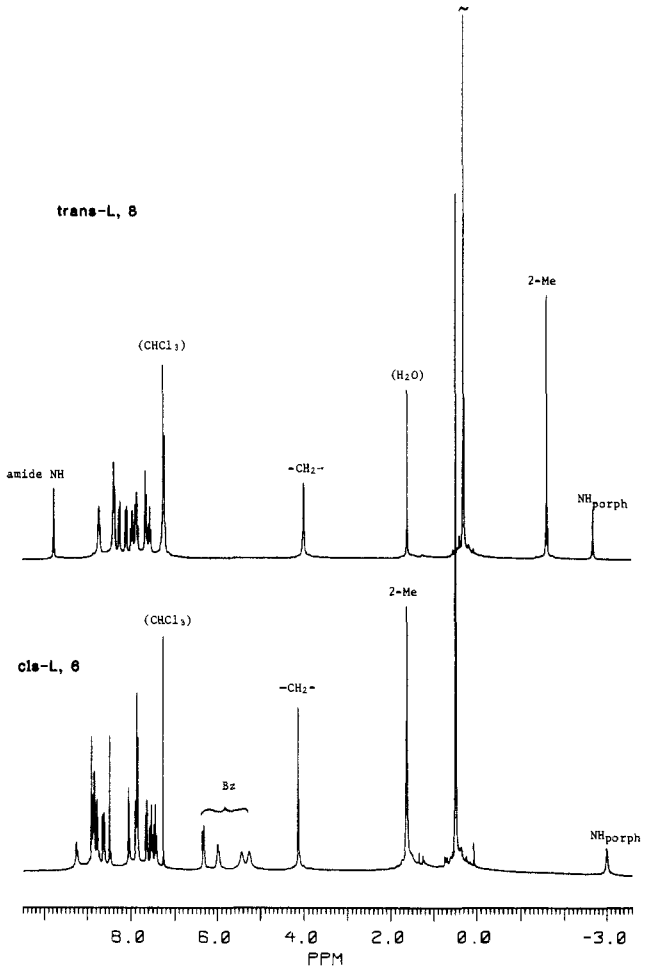

Figure 1. 270-MHz ^{1}H NMR spectra of *trans*-L **8** (upper) and *cis*-L (**6** (lower) in $CDCl_3$ at 20 °C.

imidazole appendages above the porphyrin plane. First, the 2-methyl resonance (labeled 2-Me in Figure 1) in the trans ligand is unusually upfield shifted (δ −1.61). This suggests it is experiencing a large ring current effect from the porphyrin. This is expected if the solution structure is the same as that observed in the solid-state copper complex where H bonding holds the 2-methylbenzimidazole moiety in a position which directs the 2-methyl group toward the center of the porphyrin ring (vide infra, Figure 4). Similarly, the arene protons of the 2-methylbenzimidazole moiety on the cis ligand (labeled Bz in Figure 1) are shifted markedly upfield from the normal aromatic region. This suggests that the cis ligand has the *arene* portion of the 2-methylbenzimidazole appendage rather than the 2-methyl group held over the porphyrin ring. Consistent with this difference between the trans and cis ligands is the small but significant shift of the inner porphyrinic NH protons (labeled NH_{porph} in Figure 1) in the cis ligand. This resonance is usually observed at −2.7 ppm but is apparently shifted to −3.0 ppm by the ring current effect of the benzimidazole. Finally, a two-proton resonance in the trans ligand that is distinctly downfield fo the aromatic and pyrrole region is tentatively assigned to the amide N–H protons involved in the H bonding that binds the benzimidazole moieties to the adjacent pickets. Again, this is an expected result if the solution structure of the trans ligand is the same as that observed in the solid (vide infra, Figure 6). A related deshielding of amide protons with an attendant 2-ppm downfield shift has been observed for amide H bonding to coordinated dioxygen.[49] In the L′ ligands, which have 5,6-dimethyl substitution on the benzimidazoles, *trans*-L′ shows very similar chemical shifts to *trans*-L, indicating a very similar structure. However, the NMR spectrum of *cis*-L′ shows greater similarity to the trans ligands than to *cis*-L, suggesting that the 2-methyl group of the benzimidazole lies over the porphyrin ring. The steric bulk of the 5,6-dimethyl substitution apparently prevents the arene portion of the benzimidazole from lying over the porphyrin, as seen in *cis*-L.

The temperature variations of the ^{1}H NMR spectra of the *cis*-L and *trans*-L ligands reveal some interesting complexity. Since the methylene protons of *trans*-L appear as a singlet (δ 4.0), it is apparent that the benzimidazole moieties are not rigidly locked into the hydrogen-bonded configuration found in the crystal structure. One possible dynamic process which exchanges these protons is a flipping of the benzimidazole moiety from side to side, alternately hydrogen bonding with each adjacent picket amide. As expected, at low temperature the methylene protons become diastereotopic, splitting into a set of two doublets. Similarly, the pyrrole protons undergo a temperature-dependent process. However, the alteration in the symmetry of the molecule (C_{2v} to C_2) which accounts for these spectral changes can be attributed to the freezing out of either the benzimidazole "flip" *or* the tautomerism of the inner porphyrin NH moieties. While we are unable to determine whether either or both of these processes are frozen out at low temperatures, the ΔG_{253} calculated from these spectral changes is 11.6 kcal/mol, identical with that found for the NH_{porph} tautomerism of H_2TPP.[50] The cis ligand also undergoes temperature-dependent dynamic processes, but the interpretation of the spectra is hampered by precipitation of the compound just prior to obtaining the frozen out spectrum.

Iron(III)–Porphyrin Complexes. Iron(II) can be inserted into the porphyrin moiety of the ligands directly with anhydrous $FeBr_2$. The reaction proceeds fairly quickly at room temperature, suggesting that the benzimidazole arms may accelerate the reaction rate. Certain ligand-appended porphyrins have been reported to show accelerated insertion rates relative to their nonappended counterparts.[51] The resulting iron(II)–porphyrin complexes have visible spectra which are very similar to that of Fe(TPP)[52] (TPP = *meso*-tetraphenylporphyrinate). The spectra are quite distinct from those of five- or six-coordinate imidazole-ligated species such as Fe(2-MeIm)(TPP)[52] of Fe(1-MeIm)$_2$(TPP), showing that the benzimidazole arms do not coordinate either inter- or intramolecularly. This was a purposeful design feature and derives from the use of a 2-methyl-substituted benzimidazole as well as the use of a short attachment. We have been successful in growing single crystals of a five-coordinate iron(II) complex of *trans*-L in the presence of 4-*tert*-butylimidazole, but the limited data set did not give useful metrical information.[53] It was, however, of sufficient resolution to satisfy us of its correct formulation. Its five-coordination suggests that the benzimidazole superstructure provides a significant inhibition toward six-coordination. The origin of this steric effect can be seen in the copper structure discussed below. H bonding apparently locks the benzimidazole moieties above the porphyrin ring and restricts access to the metal on one side.

Aerobic workup of the red iron(II)–porphyrin species leads to green-brown solutions which yield purple-black materials with IR and UV–vis spectroscopic properties typical of μ-oxo iron(III) dimer species. Since these porphyrins have an open face it was expected that a μ-oxo dimer would be the most stable iron(III) product. Analytically pure materials were obtained in some cases, and yet, three observations made us look more carefully at the nature of these supposed μ-oxo species. First, their magnetic moments were frequently much higher (ca. 4.2 μ_B) than that found for $[Fe(TPP)]_2O$ (ca. 2.0 μ_B). Second, the relative intensity of the ν(Fe–O) band at 865 cm^{-1} in the IR spectrum was not constant from preparation to preparation. Third, careful thin-layer chromatography always showed two mobile species of similar but distinguishable R_f values. This was puzzling because upon acidification with HCl a single pure product was observed. A subsequnt base treatment led again to two species. In the case

(49) Mispelter, J.; Momenteau, M.; Lavalette, D.; Lhoste, J.-M. *J. Am. Chem. Soc.* **1983**, *105*, 5165–5166.

(50) Abraham, R. J.; Hawkes, G. E. *Tetrahedron Lett.* **1974**, 1483–1486.

(51) See, for example: Buckingham, D. A.; Clark, C. R.; Webley, W. S. *J. Chem. Soc., Chem. Commun.* **1981**, 192–194.

(52) Collman, J. P.; Reed, C. A. *J. Am. Chem. Soc.* **1973**, *95*, 2048–2049.

(53) Scheidt, W. R.; Tate, J. R.; Reed, C. A., unpublished results.

Table II

(a) Coordinates and Standard Deviations for Cu(*trans*-L)·1.5$C_4H_{10}O$·C_7H_8

atom	*x/a*	*y/b*	*z/c*	atom	*x/a*	*y/b*	*z/c*
Cu	0.60575 (9)	0.49383 (15)	0.03905 (7)	C45	0.5165 (6)	0.6993 (12)	0.1580 (6)
N1	0.6464 (5)	0.5415 (8)	0.0168 (4)	C46	0.5288 (6)	0.6666 (11)	0.1967 (6)
N2	0.6281 (5)	0.5778 (8)	0.0842 (4)	C47	0.5548 (7)	0.5907 (12)	0.2109 (7)
N3	0.5588 (5)	0.4539 (8)	0.0566 (5)	C48	0.5666 (6)	0.5540 (10)	0.1801 (6)
N4	0.5920 (5)	0.4004 (8)	0.0011 (4)	C49	0.7200 (6)	0.7220 (10)	0.0816 (5)
C1	0.6079 (7)	0.3860 (12)	−0.0275 (6)	C50	0.7070 (6)	0.7885 (11)	0.0552 (6)
C2	0.5943 (6)	0.3069 (11)	−0.0453 (6)	C51	0.7355 (7)	0.8580 (12)	0.0668 (6)
C3	0.5692 (6)	0.2730 (11)	−0.0286 (5)	C52	0.7807 (7)	0.8608 (11)	0.1080 (6)
C4	0.5643 (6)	0.3321 (11)	−0.0009 (6)	C53	0.7969 (6)	0.7925 (10)	0.1363 (6)
C5	0.5296 (6)	0.3858 (11)	0.0416 (5)	C54	0.7659 (6)	0.7245 (10)	0.1219 (5)
C6	0.4949 (6)	0.3839 (11)	0.0570 (5)	C55	0.6381 (6)	0.4223 (10)	−0.0779 (5)
C7	0.5058 (6)	0.4486 (10)	0.0824 (5)	C56	0.5963 (7)	0.4243 (10)	−0.1207 (6)
C8	0.5458 (6)	0.4921 (12)	0.0839 (5)	C57	0.6010 (8)	0.3998 (11)	−0.1566 (7)
C9	0.6106 (6)	0.5951 (10)	0.1125 (5)	C58	0.6457 (8)	0.3835 (12)	−0.1512 (7)
C10	0.6396 (6)	0.6600 (10)	0.1421 (5)	C59	0.6875 (8)	0.3761 (12)	−0.1105 (7)
C11	0.6721 (6)	0.6814 (11)	0.1304 (6)	C60	0.6837 (7)	0.3989 (11)	−0.0714 (6)
C12	0.6638 (6)	0.6352 (11)	0.0942 (5)	N9	0.5937 (5)	0.4814 (8)	0.1933 (5)
C13	0.6760 (6)	0.6093 (11)	0.0322 (6)	N10	0.5741 (4)	0.1708 (7)	0.0533 (4)
C14	0.6943 (6)	0.6253 (11)	0.0032 (5)	N11	0.7833 (4)	0.6550 (8)	0.1495 (4)
C15	0.6777 (6)	0.5693 (11)	−0.0278 (6)	N12	0.7259 (5)	0.4005 (9)	−0.0301 (5)
C16	0.6491 (6)	0.5128 (12)	−0.0192 (6)	O1	0.5895 (4)	0.0762 (7)	0.0168 (4)
C17	0.6325 (6)	0.4409 (11)	−0.0394 (5)	O2	0.8033 (4)	0.7179 (8)	0.2135 (4)
C18	0.6867 (5)	0.6504 (10)	0.0691 (5)	O3	0.7675 (5)	0.2868 (9)	−0.0318 (4)
C19	0.5698 (6)	0.5562 (10)	0.1102 (5)	O4	0.6450 (5)	0.4961 (11)	0.2675 (5)
C20	0.5348 (6)	0.3246 (9)	0.0168 (5)	C61	0.8012 (8)	0.6537 (15)	0.1935 (8)
N5	0.5994 (6)	0.2739 (9)	0.1305 (5)	C62	0.7637 (8)	0.3446 (14)	−0.0105 (7)
N6	0.6282 (5)	0.3315 (9)	0.1980 (5)	C63	0.6060 (6)	0.1172 (11)	0.0518 (6)
N7	0.7894 (5)	0.5280 (9)	0.0926 (5)	C64	0.6328 (9)	0.4577 (15)	0.2333 (9)
N8	0.8065 (5)	0.4305 (9)	0.0574 (5)	C65	0.8161 (8)	0.5718 (13)	0.2164 (7)
C21	0.7483 (7)	0.3923 (12)	0.0857 (6)	C66	0.7735 (8)	0.5161 (15)	0.1935 (7)
C22	0.7800 (7)	0.4496 (14)	0.0780 (7)	C67	0.8352 (8)	0.5860 (13)	0.2661 (7)
C23	0.8308 (6)	0.4969 (14)	0.0570 (5)	C68	0.8634 (9)	0.5411 (14)	0.2160 (8)
C24	0.8613 (7)	0.5132 (14)	0.0997 (6)	C69	0.6585 (7)	0.1098 (12)	0.0918 (6)
C25	0.8822 (8)	0.5870 (13)	0.0447 (7)	C70	0.6851 (6)	0.1938 (11)	0.0996 (6)
C26	0.8733 (8)	0.6467 (15)	0.0684 (7)	C71	0.6865 (6)	0.0427 (10)	0.0813 (5)
C27	0.8420 (7)	0.6325 (13)	0.0854 (6)	C72	0.6539 (7)	0.0836 (12)	0.1311 (6)
C28	0.8210 (7)	0.5570 (12)	0.0796 (6)	C73	0.8065 (7)	0.3549 (12)	0.0382 (6)
C29	0.6660 (7)	0.3756 (11)	0.1528 (6)	C74	0.6597 (7)	0.3809 (12)	0.2380 (6)
C30	0.6325 (7)	0.3262 (12)	0.1602 (6)	C75	0.8120 (9)	0.3384 (12)	0.2932 (6)
C31	0.5721 (7)	0.2471 (12)	0.1488 (6)	C76	0.8579 (9)	0.3531 (12)	0.2966 (6)
C32	0.5341 (8)	0.1922 (14)	0.1339 (8)	C77	0.8705 (9)	0.3122 (12)	0.2693 (6)
C33	0.5123 (9)	0.1728 (14)	0.1581 (8)	C78	0.8373 (9)	0.2566 (12)	0.2386 (6)
C34	0.5323 (8)	0.2098 (13)	0.1998 (8)	C79	0.7915 (9)	0.2418 (12)	0.2352 (6)
C35	0.5707 (8)	0.2650 (13)	0.2174 (7)	C80	0.7789 (9)	0.2827 (12)	0.2625 (6)
C36	0.5916 (6)	0.2797 (10)	0.1911 (5)	O5	−0.0424 (8)	0.3922 (13)	0.1383 (7)
C37	0.5021 (7)	0.2527 (9)	0.0046 (6)	C81	0.5311 (9)	0.4153 (14)	0.2896 (7)
C38	0.4505 (6)	0.2590 (10)	−0.0263 (5)	C82	0.5639 (10)	0.3628 (21)	0.3272 (6)
C39	0.4210 (7)	0.1920 (12)	−0.0391 (6)	C83	−0.0075 (11)	0.4481 (17)	0.1394 (9)
C40	0.4420 (6)	0.1176 (11)	−0.0219 (5)	C84	−0.0525 (14)	0.4085 (20)	0.1731 (11)
C41	0.4919 (6)	0.1106 (11)	0.0081 (6)	O6	0.50000 (0)	0.37478 (19)	0.25000 (0)
C42	0.5225 (5)	0.1800 (10)	0.0220 (5)	C85	0.0016 (11)	0.4310 (18)	0.1025 (10)
C43	0.5546 (6)	0.5902 (10)	0.1412 (5)	C86	−0.0866 (14)	0.3461 (22)	0.1717 (12)
C44	0.5287 (6)	0.6630 (10)	0.1295 (6)	C87	0.7987 (11)	0.3812 (21)	0.3213 (11)

(b) Thermal Parameters and Standard Deviations for Cu(*trans*-L)·1.5$C_4H_{10}O$·C_7H_8

atom	U_{11}	U_{22}	U_{33}	U_{23}	U_{13}	U_{12}
Cu	0.0460 (13)	0.0328 (14)	0.0374 (13)	−0.0024 (17)	0.0270 (11)	−0.0018 (16)
N1	0.0521 (114)	0.0481 (117)	0.0226 (105)	−0.0092 (87)	0.0240 (94)	−0.0017 (94)
N2	0.0530 (111)	0.0247 (99)	0.0295 (104)	−0.0061 (84)	0.0285 (94)	−0.0112 (90)
N3	0.0344 (102)	0.0271 (102)	0.0541 (117)	−0.0067 (89)	0.0272 (96)	−0.0028 (86)
N4	0.0393 (106)	0.0379 (111)	0.0456 (112)	−0.0106 (93)	0.0317 (96)	−0.0097 (90)

atom	U_{iso}	atom	U_{iso}	atom	U_{iso}	atom	U_{iso}
C1	0.0455 (59)	C48	0.0490 (57)	C13	0.0384 (57)	C60	0.0651 (65)
C2	0.0458 (59)	C49	0.0438 (57)	C14	0.0455 (58)	N9	0.0578 (48)
C3	0.0448 (57)	C50	0.0564 (62)	C15	0.0530 (62)	N10	0.0363 (41)
C4	0.0404 (56)	C51	0.0635 (64)	C16	0.0426 (54)	N11	0.0451 (44)
C5	0.0331 (53)	C52	0.0564 (61)	C17	0.0412 (57)	N12	0.0648 (52)
C6	0.0451 (57)	C53	0.0472 (56)	C18	0.0291 (51)	O1	0.0668 (42)
C7	0.0422 (56)	C54	0.0392 (53)	C19	0.0280 (51)	O2	0.0771 (46)
C8	0.0332 (49)	C55	0.0461 (56)	C20	0.0290 (51)	O3	0.0904 (50)
C9	0.0309 (53)	C56	0.0587 (63)	N5	0.0627 (54)	O4	0.1260 (59)
C10	0.0417 (57)	C57	0.0733 (69)	N6	0.0573 (50)	C61	0.0818 (74)
C11	0.0452 (60)	C58	0.0847 (75)	N7	0.0586 (54)	C62	0.0831 (76)
C12	0.0329 (53)	C59	0.0888 (77)	N8	0.0584 (53)	C63	0.0476 (57)

Table II (Continued)

atom	U_{iso}	atom	U_{iso}	atom	U_{iso}	atom	U_{iso}
C21	0.0717 (71)	C64	0.1052 (91)	C35	0.0855 (79)	C78	0.2334
C22	0.0686 (72)	C65	0.0773 (73)	C36	0.0507 (58)	C79	0.1966
C23	0.0525 (55)	C66	0.1073 (86)	C37	0.0362 (47)	C80	0.1324
C24	0.0695 (68)	C67	0.0943 (82)	C38	0.0402 (54)	O5	0.2147
C25	0.0766 (75)	C68	0.1125 (92)	C39	0.0648 (67)	C81	0.1668
C26	0.0952 (83)	C69	0.0622 (64)	C40	0.0489 (57)	C82	0.2148
C27	0.0686 (69)	C70	0.0638 (65)	C41	0.0548 (62)	C83	0.1998
C28	0.0551 (65)	C71	0.0525 (60)	C42	0.0310 (49)	C84	0.2387
C29	0.0627 (67)	C72	0.0755 (71)	C43	0.0362 (52)	O6	0.1975
C30	0.0571 (64)	C73	0.0752 (70)	C44	0.050 (58)	C85	0.1869
C31	0.0584 (66)	C74	0.0682 (66)	C45	0.0627 (64)	C86	0.2542
C32	0.0964 (86)	C75	0.1577	C46	0.0636 (64)	C87	0.2741
C33	0.0960 (84)	C76	0.1738	C47	0.0740 (71)		0
C34	0.0925 (82)	C77	0.1861				

(c) Hydrogen Atom Coordinates for Cu(*trans*-L)·1.5$C_4H_{10}O$·C_7H_8

atom	x/a	y/b	z/c	atom	x/a	y/b	z/c
H1	0.6028	0.2796	−0.0684	H11	0.4184	0.0652	−0.0320
H2	0.5552	0.2126	−0.0345	H12	0.5081	0.0527	0.0209
H3	0.4663	0.3399	0.0495	H13	0.5183	0.6907	0.0981
H4	0.4870	0.4655	0.0997	H14	0.4965	0.7553	0.1483
H5	0.6357	0.6855	0.1683	H15	0.5192	0.6973	0.2182
H6	0.7002	0.7274	0.1461	H16	0.5646	0.5635	0.2422
H7	0.7180	0.6749	0.0062	H17	0.6723	0.7868	0.0234
H8	0.6842	0.5666	−0.0550	H18	0.7232	0.9084	0.0444
HB7	0.3683	0.0329	−0.4779	H19	0.8031	0.9145	0.1183
HB8	0.4050	−0.0998	−0.4693	H20	0.8319	0.7930	0.1679
HB9	0.3912	−0.2041	−0.4261	H21	0.5604	0.4434	−0.1264
HB10	0.3343	−0.1789	−0.3977	H22	0.5678	0.3947	−0.1893
HB11	0.5207	0.1636	0.1021	H23	0.6485	0.3761	−0.1803
HB12	0.4815	0.1311	0.1457	H24	0.7224	0.3545	−0.1063
HB13	0.5163	0.1941	0.2195	HN1	0.5809	0.4374	0.1672
HB14	0.5838	0.2943	0.2489	HN2	0.5902	0.2107	0.0815
H9	0.4340	0.3165	−0.0397	HN3	0.7820	0.5990	0.1337
H10	0.3813	0.1969	−0.0631	HN4	0.7304	0.4524	−0.0102

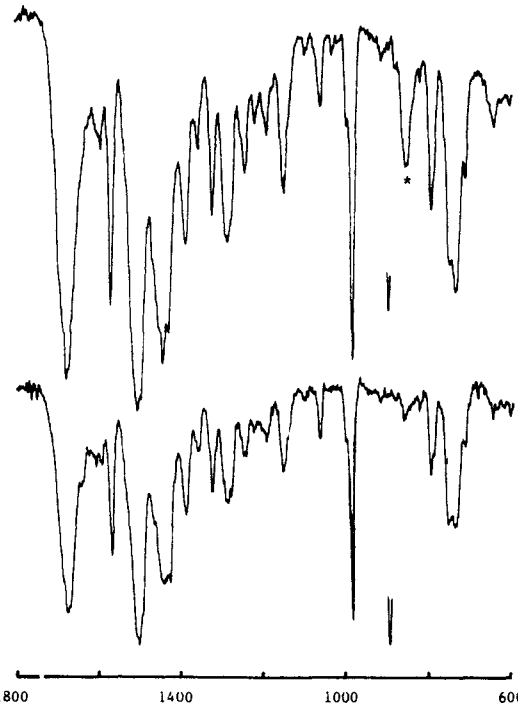

Figure 2. Infrared spectra (KBr) of the μ-oxo species O[Fe(*cis*-L)]$_2$ (upper) and the hydroxy species Fe(OH)(*cis*-L) (lower). ν(Fe–O) at 865 cm^{-1} is marked with an asterisk.

of the *cis*-L complex of iron(III) we were eventually able to achieve a reasonable separation of the two species by column chomatography and show that they spontaneously equilibrate back to the same two-component mixture over a period of a few hours. By monitoring the UV–vis spectra as the chromatography was proceeding it became clear that the slower moving species had the spectral characteristics of a μ-oxo species [λ_{max} 610, 570, 415 (Soret)] while the faster moving fraction was distinctly different [λ_{max} 625 sh, 578, 421 (Soret)]. We ascribe a monomeric hydroxide formulation, Fe(OH)(*cis*-L), to the latter species. When isolated as a purple crystalline solid, the former species shows a strong Fe–O band at 865 cm^{-1} in the IR spectrum typical of a μ-oxo iron(III) porphyrin. The latter species shows only a slight absorption at this frequency. IR spectra of both species are compared in Figure 2. No definitive assignment of a ν(O–H) band could be made in the IR spectrum of Fe(OH)(*cis*-L) presumably because of likely H-bond broadening to solvated water molecules and masking by these and the much more intense ν(N–H) vibration of the amides. The UV–vis spectra of the two species are shown in Figure 3. The symmetrical shape of the bands suggests that a clean separation has been achieved. We note, however, that the spectra are sufficiently similar that one would have considerable difficulty detecting even as much as 10–20% of one in the presence of the other. Further, the elemental compositions of the two species are very similar. (They would actually become identical if the μ-oxo species crystallized with one more water of crystallization than the hydroxo species.) This possibly explains why repeated elemental analyses were often consistent with each other and with either formulation. The high magnetic moment of the material as originally isolated is consistent with a mixture of μ-oxo dimer and hydroxo monomer since the latter is expected to be high spin.

The present interpretation is corroborated by similar observations reported while this work was in progress. The hemin hydroxide complexes of bifacially sterically hindered porphyrins such as mesityl "bis-pocket" and "strapped" tetraarylporphyrins exist only in the hydroxo form.[15,54-57] Most recently, hydroxo

(54) Cheng, R.-J.; Latos-Grazynski, L.; Balch, A. L. *Inorg. Chem.* **1982**, *21*, 2412–2418.
(55) Miyamoto, T. K.; Tsuzuki, S.; Hasegawa, T.; Sasaki, Y. *Chem. Lett. (Jpn.)* **1983**, 1587–1588.
(56) Cense, J.-M.; LeQuan, R.-M. *Tetrahedron Lett.* **1979**, 3725.
(57) Lexa, D.; Momenteau, M.; Saveant, J.-M.; Xu, F. *Inorg. Chem.* **1985**, *24*, 122–127.

Table III. Interatomic Distances (Å) (Non-Hydrogen)

		Porphine			
Cu–N(1)	1.975 (19)	N(4)–C(4)	1.416 (26)	C(9)–C(19)	1.397 (30)
Cu–N(2)	1.959 (14)	C(1)–C(2)	1.435 (27)	C(9)–C(10)	1.451 (23)
Cu–N(3)	1.981 (20)	C(1)–C(17)	1.395 (34)	C(10)–C(11)	1.327 (35)
Cu–N(4)	1.955 (15)	C(2)–C(3)	1.325 (34)	C(11)–C(12)	1.396 (30)
N(1)–C(13)	1.384 (24)	C(3)–C(4)	1.456 (32)	C(12)–C(18)	1.418 (35)
N(1)–C(16)	1.397 (30)	C(4)–C(20)	1.359 (36)	C(13)–C(18)	1.348 (30)
N(2)–C(9)	1.395 (31)	C(5)–C(20)	1.411 (30)	C(13)–C(14)	1.431 (37)
N(2)–C(12)	1.373 (25)	C(5)–C(6)	1.443 (36)	C(14)–C(15)	1.324 (28)
N(3)–C(5)	1.384 (23)	C(6)–C(7)	1.332 (27)	C(15)–C(16)	1.438 (33)
N(3)–C(8)	1.382 (30)	C(7)–C(8)	1.424 (30)	C(16)–C(17)	1.359 (27)
N(4)–C(1)	1.358 (34)	C(8)–C(19)	1.361 (25)	C(1)–C(17)	1.395 (34)
		Phenyl Rings			
C(17)–C(55)	1.488 (34)	C(44)–C(45)	1.386 (36)	C(52)–C(53)	1.427 (27)
C(55)–C(56)	1.387 (22)	C(45)–C(46)	1.326 (33)	C(53)–C(54)	1.407 (25)
C(55)–C(60)	1.377 (33)	C(46)–C(47)	1.448 (37)	C(20)–C(37)	1.492 (25)
C(56)–C(57)	1.407 (39)	C(47)–C(48)	1.449 (37)	C(37)–C(38)	1.402 (23)
C(57)–C(58)	1.334 (39)	C(18)–C(49)	1.497 (25)	C(37)–C(42)	1.364 (23)
C(58)–C(59)	1.351 (27)	C(49)–C(50)	1.371 (28)	C(38)–C(39)	1.372 (27)
C(59)–C(60)	1.494 (40)	C(49)–C(54)	1.398 (20)	C(39)–C(40)	1.395 (27)
C(19)–C(43)	1.508 (33)	C(50)–C(51)	1.392 (29)	C(40)–C(41)	1.355 (24)
C(43)–C(44)	1.403 (25)	C(51)–C(52)	1.402 (22)	C(41)–C(42)	1.420 (26)
C(43)–C(48)	1.361 (29)				
		Amide			
N(9)–C(48)	1.416 (23)	N(11)–C(54)	1.429 (22)	O(1)–C(63)	1.261 (24)
N(9)–C(64)	1.356 (27)	N(11)–C(61)	1.347 (31)	O(2)–C(61)	1.269 (31)
N(10)–C(42)	1.409 (18)	N(12)–C(60)	1.362 (21)	O(3)–C(62)	1.267 (33)
N(10)–C(63)	1.364 (27)	N(12)–C(62)	1.378 (28)	O(4)–C(64)	1.238 (37)
		Benzimidazoles			
N(5)–C(30)	1.344 (24)	C(33)–C(34)	1.405 (37)	C(21)–C(22)	1.502 (38)
N(5)–C(31)	1.384 (36)	C(34)–C(35)	1.381 (32)	C(23)–C(24)	1.399 (37)
N(6)–C(30)	1.407 (35)	C(35)–C(36)	1.403 (41)	C(24)–C(25)	1.367 (33)
N(6)–C(36)	1.353 (26)	N(7)–C(22)	1.386 (29)	C(25)–C(26)	1.421 (40)
C(29)–C(30)	1.461 (36)	N(7)–C(28)	1.378 (35)	C(26)–C(27)	1.408 (44)
C(31)–C(32)	1.372 (33)	N(8)–C(22)	1.393 (38)	C(27)–C(28)	1.391 (32)
C(32)–C(33)	1.378 (50)	N(8)–C(23)	1.353 (30)		
		Pickets			
C(61)–C(65)	1.537 (34)	C(63)–C(69)	1.509 (22)	C(62)–C(73)	1.539 (30)
C(65)–C(66)	1.474 (32)	C(69)–C(70)	1.585 (29)	C(73)–N(8)	1.436 (29)
C(65)–C(67)	1.544 (37)	C(69)–C(71)	1.582 (32)	C(64)–C(74)	1.500 (35)
C(65)–C(68)	1.572 (43)	C(69)–C(72)	1.531 (38)	C(74)–N(6)	1.482 (23)
		Solvent			
C(81)–C(82)	1.470 (34)[a]	O(5)–C(84)	1.442 (57)[a]	C(79)–C(80)	1.395[b]
O(6)–C(81)	1.382 (27)[a]	C(76)–C(77)	1.395[b]	C(80)–C(75)	1.385[b]
C(85)–C(83)	1.496 (59)[a]	C(77)–C(78)	1.395[b]	C(75)–C(76)	1.395[b]
C(84)–C(86)	1.475 (60)[a]	C(78)–C(79)	1.395[b]	C(75)–C(87)	1.446[a]
O(5)–C(83)	1.423 (45)[a]				

[a] Constrained refinement. [b] Rigid group of refinement.

and μ-oxo forms of ligand-appended hemins that are quite closely related to the present system have been reported.[29] Their UV–vis spectra are very similar to the analogous species in our work and, like the present species, all λ_{max} values of the monomeric species are red-shifted relative to the dimeric species.

The stabilization of a monomeric hydroxo species with the present ligands could derive in part from the steric inhibition of the bulky appendages. However, the porphyrins do have an open face where there is no inhibition to dimerization. Since some of the hydroxo species is always present in an equilibrated mixture, we conclude that the appendages to the porphyrin must offer some dipolar stabilization of the hydroxide ligand within the cavity of the superstructure. A similar observation has been made with an iron(III) "nicotinamide picket" porphyrin.[38] A preference for anion binding within the pocket of picket fence porphyrins can be seen in structural studies of Weiss et al.,[58] and this suggests that it is the ortho amido linkages that offer the dipolar stabilization of polarized ligation on the hindered side of the porphyrin. This feature may prove to be very useful in future work with anion-bridged dinuclear complexes.

X-ray Structure of Copper(II) Complex. The ligand system was designed to have enough rigidity and symmetry to crystallize nicely but not so much as to become insoluble. This trade-off of workable solubility vs. ability to crystallize is a very important consideration in metalloporphyrin synthesis. Few "tailed" porphyrins have yielded to single-crystal analysis,[8,59] and many of the more symmetrical face-to-face porphyrin dimers[16-18] have markedly limited solubilities when compared to their monomers. These properties can be understood not only in terms of size but also in terms of entropic factors such as degrees of rotational freedom and numbers of identical orientations for efficient crystal packing. We had anticipated that the inherent floppiness of any moiety appended via a freely rotating methylene group (such as in our ligands) would be offset by a tendency of the benzimidazoles to lie more of less coplanar with the porphyrin ring. We also anticipated that the *tert*-butyl groups would fill voids in the superstructure, making the molecule block-shaped overall for good

(58) Schappacher, M.; Ricard, L.; Weiss, R.; Montiel-Montaya, R.; Gonser, U.; Bill, E.; Trautwein, A. *Inorg. Chim. Acta* **1983**, *78*, L9–L12.

(59) Bobrik, M. A.; Walker, F. A. *Inorg. Chem.* **1980**, *19*, 3383–3390.

Table IV. Selected Bond Angles (deg)

Porphine							
N(1)-C(13)-C(14)	108.0 (18)	C(8)-C(19)-C(9)	125.0 (22)	C(1)-C(2)-C(3)	108.3 (22)	N(1)-C(13)-C(18)	125.1 (23)
N(1)-C(16)-C(15)	107.5 (17)	N(3)-C(8)-C(19)	125.5 (20)	C(2)-C(1)-N(4)	110.3 (20)	C(14)-C(13)-C(18)	126.9 (19)
C(13)-N(1)-C(16)	107.1 (19)	C(7)-C(8)-C(19)	126.4 (22)	C(1)-N(4)-C(4)	105.7 (17)	Cu-N(2)-C(9)	128.6 (12)
C(14)-C(15)-C(16)	108.3 (23)	N(3)-C(8)-C(7)	107.9 (16)	C(2)-C(1)-C(17)	124.3 (24)	Cu-N(2)-C(12)	127.6 (16)
C(13)-C(14)-C(15)	108.9 (20)	C(6)-C(7)-C(8)	110.7 (22)	N(4)-C(1)-C(17)	125.3 (19)	N(2)-C(9)-C(20)	123.1 (16)
C(13)-C(18)-C(12)	123.7 (18)	C(5)-C(6)-C(7)	104.8 (19)	C(1)-C(17)-C(16)	123.1 (23)	C(8)-C(19)-C(43)	121.3 (19)
N(1)-C(13)-C(18)	125.1 (23)	N(3)-C(5)-C(6)	110.5 (18)	N(1)-C(16)-C(17)	107.5 (17)	C(9)-C(19)-C(43)	113.8 (15)
C(9)-C(19)-C(8)	125.0 (22)	C(5)-N(3)-C(8)	105.8 (18)	C(15)-C(16)-C(17)	125.6 (23)	Cu-N(3)-C(5)	127.5 (16)
N(2)-C(12)-C(18)	124.9 (17)	C(6)-C(5)-C(20)	124.6 (18)	N(1)-Cu-N(2)	89.9 (7)	Cu-N(3)-C(8)	126.5 (12)
C(11)-C(12)-N(2)	111.2 (21)	N(3)-C(5)-C(20)	124.8 (21)	N(1)-Cu-N(3)	173.6 (5)	C(4)-C(20)-C(37)	117.9 (19)
C(10)-C(11)-C(12)	109.0 (17)	C(4)-C(20)-C(5)	122.7 (18)	N(2)-Cu-N(3)	89.9 (7)	C(5)-C(20)-C(37)	118.9 (21)
C(9)-C(10)-C(11)	105.8 (20)	N(4)-C(4)-C(20)	126.5 (19)	N(1)-Cu-N(4)	90.7 (7)	Cu-N(4)-C(4)	126.4 (16)
C(9)-N(2)-C(12)	103.8 (15)	C(3)-C(4)-C(20)	125.4 (18)	N(2)-Cu-N(4)	171.2 (5)	Cu-N(4)-C(1)	105.7 (17)
N(2)-C(9)-C(19)	123.1 (16)	C(3)-C(4)-N(4)	107.9 (21)	N(3)-Cu-N(4)	90.4 (7)	N(1)-C(16)-C(15)	107.5 (17)
C(10)-C(9)-C(19)	127.0 (22)	C(2)-C(3)-C(4)	107.4 (18)	Cu-N(1)-C(16)	125.0 (12)		
Phenyl Rings							
C(16)-C(17)-C(55)	118.1 (21)	C(13)-C(18)-C(49)	118.6 (21)	C(54)-C(49)-C(50)	116.6 (17)	C(20)-C(37)-C(42)	120.3 (15)
C(1)-C(17)-C(55)	118.6 (17)	C(12)-C(18)-C(49)	117.3 (18)	C(19)-C(43)-C(44)	117.9 (18)	C(37)-C(38)-C(39)	119.9 (16)
C(17)-C(55)-C(56)	119.6 (20)	C(18)-C(49)-C(50)	122.6 (14)	C(19)-C(43)-C(48)	122.3 (16)	C(38)-C(39)-C(40)	120.4 (17)
C(17)-C(55)-C(60)	120.6 (15)	C(18)-C(49)-C(54)	120.8 (16)	C(43)-C(44)-C(45)	120.3 (19)	C(39)-C(40)-C(41)	120.3 (18)
C(55)-C(56)-C(57)	119.1 (21)	C(49)-C(50)-C(51)	124.4 (15)	C(44)-C(45)-C(46)	121.3 (19)	C(40)-C(41)-C(42)	119.5 (17)
C(56)-C(57)-C(58)	121.6 (18)	C(50)-C(51)-C(52)	118.5 (18)	C(45)-C(46)-C(47)	121.8 (24)	C(41)-C(42)-C(37)	120.3 (14)
C(57)-C(58)-C(59)	122.2 (29)	C(51)-C(52)-C(53)	119.6 (17)	C(46)-C(47)-C(48)	115.5 (21)	C(42)-C(37)-C(38)	119.6 (16)
C(58)-C(59)-C(60)	117.1 (25)	C(52)-C(53)-C(54)	118.2 (14)	C(47)-C(48)-C(43)	121.3 (18)	N(10)-C(42)-C(37)	121.6 (15)
C(59)-C(60)-C(55)	119.5 (16)	C(53)-C(54)-C(49)	122.6 (16)	C(48)-C(43)-C(44)	119.7 (21)	N(10)-C(42)-C(41)	118.1 (14)
C(60)-C(55)-C(56)	119.7 (23)			C(20)-C(37)-C(38)	120.0 (15)		
Benzimidazole							
N(5)-C(30)-C(29)	124.3 (23)	C(35)-C(36)-C(31)	122.8 (19)	N(8)-C(22)-C(21)	125.0 (21)	C(24)-C(23)-C(28)	120.2 (22)
N(6)-C(30)-C(29)	124.3 (17)	C(35)-C(31)-C(32)	118.7 (26)	C(22)-N(7)-C(28)	105.1 (21)	C(23)-C(28)-C(27)	120.6 (25)
C(30)-N(5)-C(31)	105.1 (20)	C(36)-N(6)-C(30)	106.2 (16)	N(7)-C(28)-C(23)	109.8 (19)	C(23)-N(8)-C(22)	107.7 (19)
C(31)-C(32)-C(33)	122.1 (25)	C(36)-C(31)-N(5)	109.7 (17)	C(28)-C(27)-C(26)	117.9 (24)	C(73)-N(8)-C(22)	126.5 (20)
C(32)-C(33)-C(34)	116.5 (24)	C(36)-N(6)-C(74)	127.5 (21)	C(27)-C(26)-C(25)	121.5 (23)	C(73)-N(8)-C(23)	125.7 (23)
C(33)-C(34)-C(35)	125.2 (31)	C(30)-N(6)-C(74)	126.2 (18)	C(26)-C(25)-C(24)	119.2 (27)	C(28)-C(23)-N(8)	107.1 (22)
C(34)-C(35)-C(36)	114.5 (23)	N(7)-C(22)-C(21)	124.8 (25)	C(25)-C(24)-C(23)	120.5 (24)	N(8)-C(23)-C(24)	132.7 (23)
Picket							
C(37)-C(42)-(10)	121.6 (15)	C(63)-C(69)-C(71)	107.7 (16)	C(53)-C(54)-N(11)	118.0 (13)	C(61)-C(65)-C(67)	106.8 (19)
C(41)-C(42)-N(10)	118.1 (14)	C(63)-C(69)-C(72)	107.4 (20)	C(54)-N(11)-C(61)	125.2 (17)	C(61)-C(65)-C(68)	108.4 (24)
C(42)-N(10)-C(63)	127.2 (14)	C(70)-C(69)-C(71)	111.6 (19)	N(11)-C(61)-O(2)	119.7 (21)	C(66)-C(65)-C(67)	115.1 (25)
N(10)-C(63)-O(1)	117.4 (14)	C(70)-C(69)-C(72)	112.7 (17)	N(11)-C(61)-C(65)	116.7 (21)	C(66)-C(65)-C(68)	111.9 (21)
N(10)-C(63)-C(69)	118.6 (17)	C(71)-C(69)-C(72)	109.4 (16)	O(2)-C(61)-C(65)	123.6 (23)	C(67)-C(65)-C(68)	104.5 (17)
C(63)-C(69)-C(70)	107.7 (15)	C(49)-C(54)-N(11)	119.4 (15)	C(61)-C(65)-C(66)	109.8 (16)		
Amides							
C(55)-C(60)-N(12)	121.0 (23)	N(12)-C(62)-O(3)	123.0 (18)	C(43)-C(48)-N(9)	121.1 (21)	N(9)-C(64)-O(4)	120.8 (24)
C(59)-C(60)-N(12)	119.4 (22)	N(10)-C(63)-C(69)	118.6 (17)	C(47)-C(48)-N(9)	117.5 (18)	O(4)-C(64)-C(74)	118.0 (20)
C(60)-N(12)-C(62)	128.3 (19)	O(1)-C(63)-C(69)	123.9 (20)	C(48)-N(9)-C(64)	130.8 (18)	N(9)-C(64)-C(74)	121.0 (20)
Solvent							
C(86)-C(84)-O(5)	108.0 (29)[a]	O(5)-C(83)-C(85)	109.9 (25)[a]	C(82)-C(81)-O(6)	113.9 (23)[a]		
C(84)-O(5)-C(83)	110.8 (25)[a]			C(81)-O(6)-C(81)	121.6 (31)[a]		

[a] Constrained during refinement.

crystallization but at the same time lending good organic solvent solubility to the molecule.

These features have been realized in the isolation of Cu(*trans*-L) which crystallizes as a 1.5 diethyl ether/toluene solvate. The atom numbering scheme used in the X-ray structure determination is shown in the perspective view of Figure 4. The atomic coordinates and thermal parameters are listed in Table IIa-c. As seen in Figure 4, the molecule displays an approximate twofold axis of symmetry perpendicular to the porphyrin plane. The porphinato ring is distorted from planarity to approximate S_4 symmetry in a manner similar to that found for the copper(II) tetraphenylporphinato structure.[60] This is best seen in the side-on view of Figure 5. The normals to the copper–pyrrole planes trans to each other intersect at 15° and 16°, respectively, while those of adjacent copper–pyrrole planes range from 10° to 12°. This ruffling of the core is probably a response to having a somewhat smaller metal than is optimum for a relaxed planar core.[61] The CuN_4 coordination unit also possesses S_4 symmetry with the nitrogen atoms displaced ca. 0.12 Å about the mean plane. The average Cu–N bond length is 1.968 (13) Å, which agrees well with that found in Cu(TPP) (1.981 (7) Å).[60] Other bond lengths are listed in Table III, and selected bond angles are listed in Table IV.

The benzimidazole rings in the superstructure of the porphyrin adopt a stacked plane configuration (Figure 5). The normals to the planes of the two benzimidazoles and the porphyrin are 16.2° and 20.7°, respectively. The distance of the closet approaching atoms of the benzimidazole moieties to the mean plane of the porphyrin ring ranges from 2.8 to 3.8 Å, indicating that some π–π interaction may be present. However, the orientation of the benzimidazole moieties above the porphyrin is probably dictated by hydrogen bonding of a pivalamide picket N–H to its adjacent benzimidazole N donor. This is illustrated in Figure 6. The

(60) Fleischer, E. B.; Miller, C. K.; Webb, L. E. *J. Am. Chem. Soc.* **1964**, *86*, 2342–2347.

(61) Scheidt, W. R. *Acc. Chem. Res.* **1977**, *10*, 339–345.

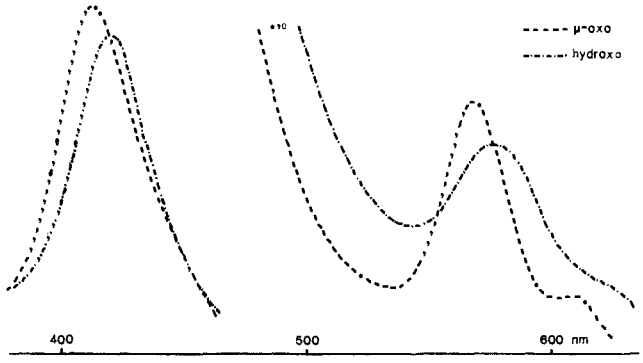

Figure 3. Visible spectra of the μ-oxo species O[Fe(*cis*-L)]$_2$ (---) and the hydroxy species Fe(OH)(*cis*-L) (···) immediately after separation by chromatography.

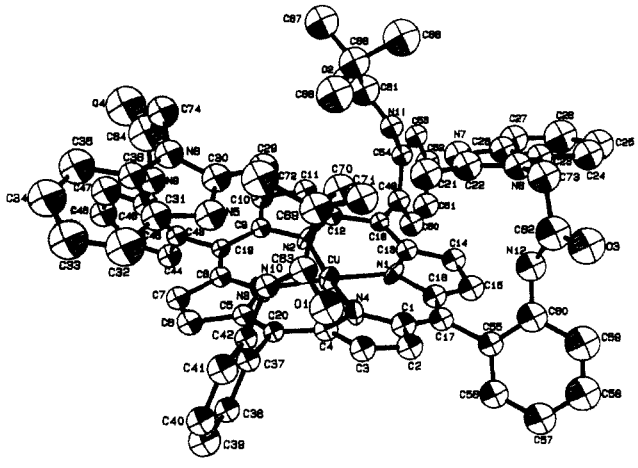

Figure 4. Perspective view and atom numbering scheme used for Cu(*trans*-L).

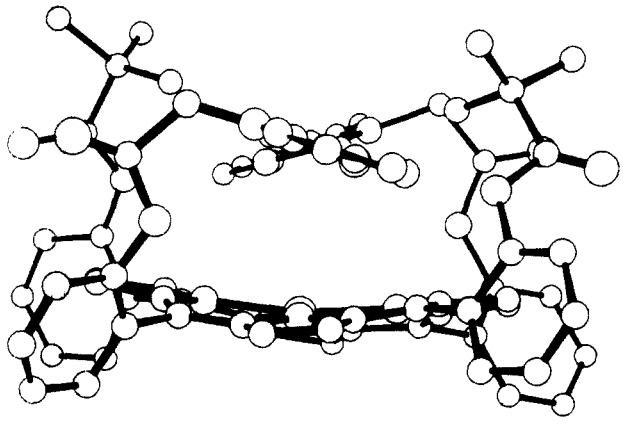

Figure 5. Side-on perspective view of Cu(*trans*-L).

N11–N7 distance is 3.00 Å, which is only slightly longer than a value typical of strong associative hydrogen bonding in secondary amides (2.8–2.9 Å).[62] The existence of this hydrogen bond probably explains the unusually large distortion of the amido

(62) Hamilton, W. C.; Ibers, J. A. *Hydrogen Bonding in Solids*; W. A. Benjamin: New York, 1968.

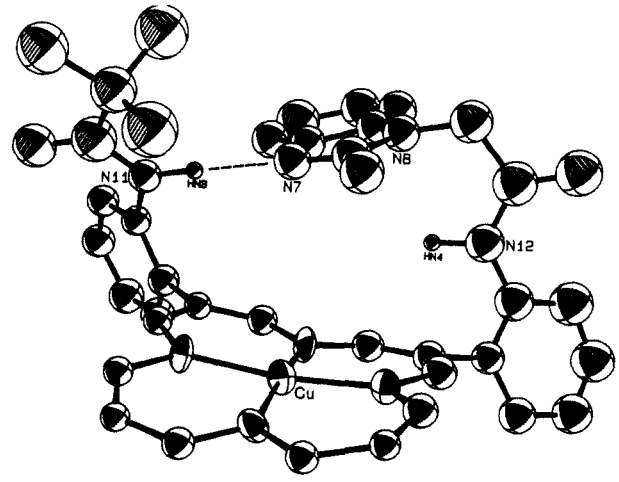

Figure 6. A detail from the structure of Cu(*trans*-L) showing H bonding of a picket amide to an adjacent benzimidazole.

groups from planarity with their phenyl groups. For the N11 pivalamido group illustrated in Figure 6, the torsional angle between the amide plane and the phenyl ring is 49°. The N12 amide plane which is part of the connection to the benzimidazole is rotated 45° from the plane of its porphinate phenyl group. It seems clear that the intramolecular hydrogen bonding is formed at the expense of π-delocalization which otherwise might be expected to keep the anilide moiety planar.

Conclusion

Bis-ligand-appended porphyrins with useful design features and good handling characteristics are synthetically accessible and amenable to X-ray crystallographic characterization. Their potential as binucleating ligands is now being explored with the encouraging prospect of definitive structural characterization.

Acknowledgment. This work was supported by the National Institutes of Health (GM 23851).

Registry No. **1**, 68070-27-9; **2**, 104070-00-0; **3**, 104070-01-1; **4**, 104070-02-2; **5**, 90703-83-6; **6**, 104070-03-3; **7**, 104089-94-3; **8**, 104070-04-4; 9, 104070-05-5; $BrCH_2C(O)OMe$, 96-32-2; Fe(OH)(*cis*-L), 104070-12-4; Fe_2O(*cis*-L), 104070-13-5; Cu(*trans*-L′), 104070-14-6; Cu(*trans*-L), 104070-15-7; Cu(*trans*-L)·1.5Et_2O·PhMe, 104153-49-3; (α,α,α,α)-15-[*o*-[(triphenylmethyl)amino]phenyl]-5,10,20-tris(*o*-aminophenyl)-21*H*,23*H*-porphine, 85294-22-0; (α,α,α,α)-5,15,20-tris[*o*-[(triphenylmethyl)amino]phenyl]-10-(*o*-aminophenyl)-21*H*,23*H*-porphine, 104070-06-6; (α,α,α,α)-5-[*o*-[(2,2-dimethyl-1-oxopropyl)amino]phenyl]-10,15,20-tris(*o*-aminophenyl)-21*H*,23*H*-porphine, 85294-19-5; 2-methyl-1*H*-benzimidazole, 615-15-6; methyl 2-(2-methyl-1*H*-benzimidazol-1-yl)acetate, 2033-54-7; 2-(2-methyl-1*H*-benzimidazol-1-yl)-acetic acid hydrobromide, 104070-07-7; 2-(2-methyl-1*H*-benzimidazol-1-yl)acetyl chloride, 104070-08-8; (α,α,α,α)-5,10,15-tris[*o*-[(2,2-dimethyl-1-oxopropyl)amino]phenyl]-20-(*o*-aminophenyl)-21*H*,23*H*-porphine, 75557-89-0; (α,α,α,α)-5,10,15,20-tetrakis[*o*-[(2,2-dimethyl-1-oxopropyl)amino]phenyl]-21*H*,23*H*-porphine, 55253-62-8; 2,5,6-trimethyl-1*H*-benzimidazole, 3363-56-2; methyl 2-(2,5,6-trimethyl-1*H*-benzimidazol-1-yl)acetate, 104070-09-9; 2-(2,5,6-trimethyl-1*H*-benzimidazol-1-yl)acetic acid hydrobromide, 104070-10-2; 2-(2,5,6-trimethyl-1*H*-benzimidazol-1-yl)acetyl chloride, 104070-11-3.

Supplementary Material Available: Table of observed and calculated structure factors (11 pages). Ordering information is given on any current masthead.